Rotation, translation, charge transfer, and electronic structure of C_{60} on Cu(111) surface

Lin-Lin Wang and Hai-Ping Cheng

Department of Physics and Quantum Theory Project, University of Florida, Gainesville, Florida 32611, USA

The energetics and electronic structure of a C_{60} monolayer on Cu(111) surfaces have been investigated thoroughly via large-scale first-principles density functional theory. The calculated adsorption site and orientation of the molecule, and the work function are in excellent agreement with experimental observations. We find that the translational motion of C_{60} across Cu-Cu bonds can be barrierless, while a 360°, on-site rotational motion is subject to a barrier of 0.3 eV. A close to $0.8e^-$ charge transfer per molecule from the surface to the C_{60} monolayer is determined, which provides important insights into a number of experimental measurements. Our analysis also indicates that the transferred electrons are localized in a plane between the molecule and surface, and that the bands near the Fermi level are highly hybrid between the surface and the molecule, reflecting a strong metal-fullerene coupling. Furthermore, an analysis of the dipole moment clarifies the puzzling phenomenon regarding the work function.

PACS number(s): 73.61.Wp, 73.25.+i, 73.20.At

I. INTRODUCTION

Metal-surface–C_{60} interaction has been studied extensively in experiments in the past decade. Due to the high electron affinity of C_{60} molecules as well as the metallic nature of the surfaces, charge transfer has been observed in a number of systems such as C_{60} adsorbed on metal Cu, Ag, and Au (while some controversy exists about C_{60} on an Al surface).[1–6] Modification in the electronic structure of the molecules is found to be responsible for the enhancement in Raman spectroscopy[7–11] and changes in resistance.[3,12–14] Lately, angle-resolved photoemission spectroscopy (ARPES) has been reported to study band dispersion in an electron-doped (via alkali-metal) C_{60} monolayer (ML) on Ag surfaces.[15] Unlike a Si surface in which charge transfer is found to be small,[16,17] it is suggested that electrons from a metal surface are likely to transfer to the lowest unoccupied molecule orbital (LUMO) of a C_{60}, which is a threefold degenerate level with a symmetry labeled as t_{1u}. The charge transfer leads to strong interactions between metal surfaces and fullerene molecules.

The C_{60}-Cu film is a system in which fascinating phenomena have been observed in studies of conductance as a function of the thickness of the copper film.[3,8,10,18,19] Experiments[3] indicate that when a C_{60} ML is placed on top of a thin film, the resistance of a given sample is measured about 8000 Ω, which leads to a resistivity corresponding to half the three-dimensional alkali-metal-doped compounds A_3C_{60} (A = K, Rb). When the C_{60} is beneath the Cu film, the ML also enhances the conductance. It is suggested from experimental analysis that the enhancement of conductance in the C_{60}-Cu systems is due to charge transfer from Cu to C_{60} at the interface.

Further experimental measurements indicate that when the thickness of the Cu film increases, the resistance curves cross.[3] As the thickness of the Cu film increases, the conductance of the film increases to approach the bulk Cu limit, which is much higher than the conductance of the electron-doped C_{60}. When the thick Cu film is covered with a C_{60} ML, the resistance of the system increases. This phenomenon

is understood as a result of a diffusive surface scattering process.[3]

Despite the large amount of experimental data on electronic, transport, and optical properties, there are many basic problems, such as the number of electrons transferred from the surface to the C_{60} molecules (different experiments have given different values[8,9,20]). Models that apply successfully to one metal surface can give completely unphysical conclusions for another. The work function of a variety of C_{60}-covered metal surface remains to be understood; the pure and C_{60}-covered Cu(111) have similar work functions, and the simple dipole model fails to explain this behavior.[21] To date, except for a recent band structure study of an alkali-metal-doped K_3C_{60} monolayer film on a Ag(111) surface has been reported to explain the experimental measurement (via angle-resolved photoemission) of band dispersion and charge transfer from alkali metal to C_{60},[15] there is no full first-principles theoretical calculation that provides a complete description of the system.

In this paper, we report our work on C_{60}-Cu(111) interactions. We address a collection of issues raised in a decade of experimental work, such as C_{60} adsorption sites and orientation, barriers to translation and rotation on the surface, surface deformation, work functions, charge transfer, density of states (DOS), and electronic band structure.

II. THEORY, METHOD, AND COMPUTATIONAL DETAILS

The calculations have been performed within the framework of density functional theory (DFT) with local density approximation (LDA).[22] A plane-wave basis set in conjunction with the Vanderbilt ultrasoft pseudopotential[23] are used within the VASP code.[24] The Kohn-Sham equation is

$$\left[-\frac{1}{2}\nabla^2 + V(\rho(\mathbf{r})) \right]\psi_\alpha(\mathbf{r}) = \varepsilon_\alpha \psi_\alpha(\mathbf{r}), \quad \alpha = (i,k), \quad (1)$$

$$\psi_\alpha(\mathbf{r}) = \psi_{i,k}(\mathbf{r}) = \sum_{\mathbf{G}, 1/2 |\mathbf{G}+\mathbf{k}|^2 \leqslant E_{cut}} c_{i,\mathbf{G}+\mathbf{k}} e^{i(\mathbf{G}+\mathbf{r})\cdot\mathbf{r}}, \quad (1a)$$

TABLE I. Calculated and experimentally measured properties of Cu(111) surface. The numbers in paren-thesis are obtained using GGA. The last three quantities Δd_{ij} are percentage changes of interlayer spacing of the first four layers with respect to the bulk spacing.

Lattice constant (Å)		Cohesive energy (eV)	Bulk modulus (GPa)		
Calc.	3.53 (3.64)	4.75(3.77)	188 (141)		
Expt.	3.61[a]	3.50[b]	142[c]		
Work function (eV)		Surface energy (eV)	Δd_{12}	Δd_{23}	Δd_{34} (%)
Calc.	5.24 (4.86)	0.60(0.48)	-0.92	-0.11	0.17
Expt.	4.94[d]		-0.7[e]		

[a]Reference 29.
[b]Reference 30.
[c]Reference 31.
[d]Reference 32.
[e]Reference 33.

$$\rho(\mathbf{r}) = \sum_{\alpha}^{N} f_{\alpha} |\psi_{\alpha}(\mathbf{r})|^2, \tag{1b}$$

for each orbital, and each k point is solved self-consistently. In Eq. (1), $\alpha = (i,k)$ are indices of orbital and k point, $\mathbf{G}$ are reciprocal lattice vectors, and f_{α} is the occupation number. The Monkhorst-Pack mesh[25] is used to take advantages of symmetry of the Brillouin zone.

To analyze the obtained electronic structure, the density of states and energy bands are projected onto the C_{60} molecule and Cu surface via the equations

$$p_{\mu,i} = \sum_{k} w_k |\langle \phi_{\mu,k}(\mathbf{r}) | \Psi_{i,k}(\mathbf{r}) \rangle|^2 \tag{2a}$$

and

$$DOS_{\mu}(\varepsilon) = \sum_{k} w_k \sum_{i} \delta(\varepsilon - \varepsilon_{i,k}) |\langle \phi_{\mu,k}(\mathbf{r}) | \Psi_{i,k}(\mathbf{r}) \rangle|^2, \tag{2b}$$

respectively. In Eqs. (2), $\phi_{\mu,k}$ and $\Psi_{i,k}(\mathbf{r})$ are atomic and Bloch state wave functions, respectively, w_k is the weight of each k point, and the indices μ and (i,k) are labels for atomic orbitals and Bloch states, respectively. The projection provides a useful tool for analyzing the band structure and the density of states.

Finally, we introduce a general approach used by Michaelides et al.[26] to estimate the change in dipole moment upon molecular adsorption on surfaces as

$$\Delta \mu = \int_{-a}^{-a+z_0/2} z \Delta \sigma(z) dz, \tag{3}$$

with

$$\Delta \sigma(z) = \int_{unit\ cell} \Delta \rho(\mathbf{r}) dx\, dy \tag{3a}$$

and

$$\Delta \rho = \rho(C_{60} + Cu) - \rho(C_{60}) + \rho(Cu). \tag{3b}$$

Note that in Eq. (3), a is the distance from the center of the slab to the top of the surface layer, $z_0/2$ is half the length of the unit cell in the z direction, the change of dipole moment induced by molecule-surface interaction at the interface is complicated in general, which cannot be simply estimated as a product of the charge transfer and the distance between C_{60} and the surface.

The Cu slab is constructed using a 7-layer (4×4) surface unit cell, which contains 112 Cu atoms. The vacuum region between two slabs is chosen to be 22 Å in thickness to minimize artifacts. The total number of electrons in the unit cell, including 240 electrons from the C_{60} molecule, is 1472. The k mesh is $3 \times 3 \times 1$. The cutoff energy for plane-wave expansion is 21 Ry, which, together with k-mesh and vacuum thickness, is tested to give satisfactory total energy (1 meV/ atom) and force (0.02 eV/Å at equilibrium) convergence. In our simulations, the top four layers are allowed to relax and the bottom three layers are held at fixed bulk positions.

III. RESULTS

We first perform testing calculations on a pure Cu(111) surface whose properties are well known. Table I lists results from simulations and experiments. As expected, results from the generalized gradient correction (GGA)[27,28] are, in general, in better agreement with the observed values. The cohesive energy and bulk modulus from LDA[22] calculation are 25% off, but the work function and lattice constant are pretty good compared to the measured data. As we derive binding energies from the difference between a C_{60}-covered Cu(111) surface and a bare Cu(111) plus a C_{60} ML, or compare binding energies among different adsorption sites, error cancellations further increases the accuracy of the LDA (see later discussion). Band structure and the DOS are not sensitive to the level of approximations made in this study at all. Major conclusions from this study are not influenced by LDA.

A. Energy landscape

Experiments[19,34−36] proposed that the C_{60} is lying on a hexagonal face at a threefold on-hollow site of the Cu(111) surface lattice [Fig. 1(a)]. Our calculations first confirm that
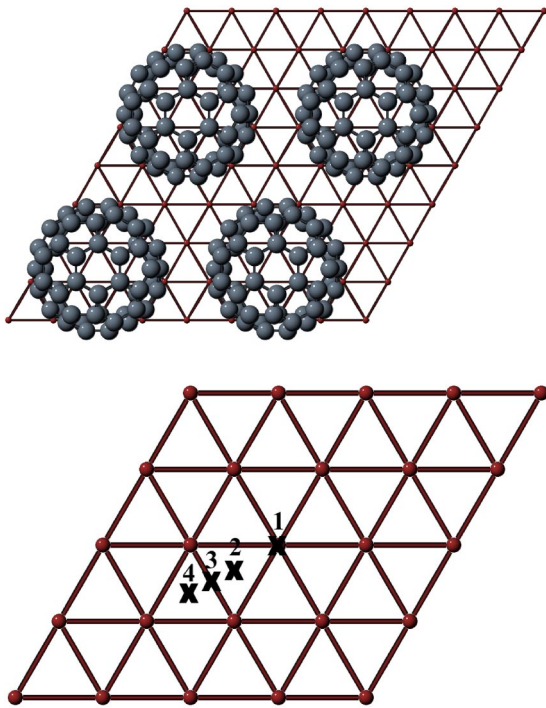
FIG. 1. (a) C_{60} molecules on hcp sites in the (4×4) unit cells with lowest energy (4 cells are shown); and (b) adsorption sites on a Cu(111) surface: 1, on-top; 2, fcc; 3, bridge; and 4, hcp. Sites 2 and 4 are not equivalent because of the differences in lower surface layers (not shown).

this is a more stable situation than the one lying on a pentagonal face. However, there are two different on-hollow sites, hcp and fcc, which cannot be determined experimentally. Our calculations indicate that the hcp site is the lowest energy state (by only 0.02 eV). We further investigate four potential binding sites, hcp, fcc, bridge and on-top [Fig. 1(b)] for this stable binding geometry, with various orientations of the hexagonal with respect to the Cu(111) lattice (Fig. 2). We
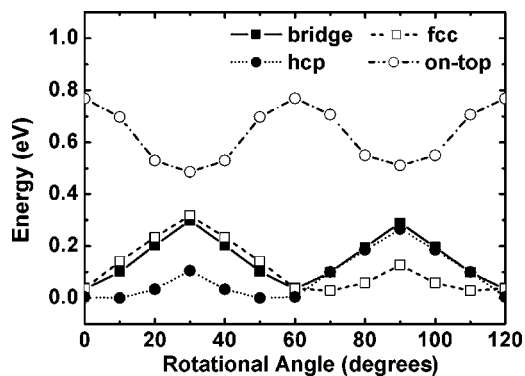

FIG. 2. Energy as functions of orientation for all four sites shown in Fig. 1(b). Zero angle orientation is defined as in Fig. 1(a). The system has a threefold symmetry because of the Cu lattice. When the angle is $0°$, $60°$, $120°$,…, the hcp (filled circle), bridge (filled square), and fcc (open square) sites but not the on-top (open circle) site have similar energy. A C_{60} molecule can translate from one site to another, among hcp, fcc, and bridge, freely with exception to the on-top site.

have found that the hcp site is indeed the most stable one, but followed very closely by the bridge, and then fcc and on-top sites. It can be seen in Fig. 2 that a C_{60} molecule can easily move via translational motion from one hcp site to another with a nearly zero barrier (translate from hcp to bridge, to fcc and then to hcp), or via rotation with a $360°$ on-site (hcp, fcc, and bridge) rotational energy barrier of 0.3 eV. Note that a $60°$ on-site (hcp and fcc) rotation is subjected to a barrier at $30°$ of only 0.1 eV. These energetic features determine the diffusion of C_{60} molecules on Cu(111) surfaces. Experiments have found that C_{60} is extremely mobile on a Cu surface,[37] which is a result of the low-energy barrier when the molecule rotates and translates simultaneously. An analysis of the density of states for these adsorption sites will be presented in later section.

The calculated binding energy (BE) of C_{60} and Cu(111) on a hcp site is 2.24 eV, followed by bridge at 2.22 eV, fcc at 2.22 eV, and on-top at 2.00 eV. Although LDA tends to overestimate the BE for all systems as observed in bulk Cu, the error in the C_{60}-Cu(111) binding is probably small in this system. So far, there is no data reported for C_{60} desorption energy from Cu(111), but the experimental desorption energy of a C_{60} molecule from a Au(111) surface is 1.87 eV,[20] which is estimated to be smaller than that from a Cu surface. We conclude that the expected BE of C_{60}-Cu(111) is between 1.9 and 2.2 eV.

B. Structure modification

The C_{60}-Cu(111) interaction modifies the Cu lattice as follows: At the C_{60}-Cu(111) contact, the Cu-Cu bond length in the triangle right underneath the molecule expands by 5–6 % (very significant), and the short and long C-C bonds in the C_{60} hexagon right above the Cu surface increase by 3% and 2% (not negligible); the Cu atoms beneath the molecule lower their position by 0.14 Å, and Cu atoms surrounding the molecule rise by 0.10 Å, with respect to the average atomic position in the surface layer. The deformation and the perturbation from the molecule cause electrons in the surface to undergo diffusive reflection when they encounter the interface, thus reducing the conductance of a relatively thick metal film.

C. DOS and band hybridization

The electronic DOS and partial DOS projected on Cu and C_{60} of the hcp site are shown in Fig. 3. It can be seen that the DOS near the Fermi level is dominated by states from the Cu(111) surface [panel (b)]. The Fermi level is located above the region of the strong d band. At low energy (<8 eV), the DOS is modulated by the feature of a C_{60} ML [see the sharp peaks in Fig. 3(a)]. The partial DOS projected on the surface of the C_{60} ML [Fig. 3(c), dashed line] is compared to an isolated C_{60} ML [Fig. 3(c), solid line]. Relative to an isolated C_{60} layer, energy levels near the Fermi energy of the absorbed C_{60} layer have shifted to lower energy as a result of molecule-surface interaction. The LUMO t_{1u}-derived band is now broadened and partially filled (below E_F) due to the surface-to-molecule charge transfer. The calculated DOS
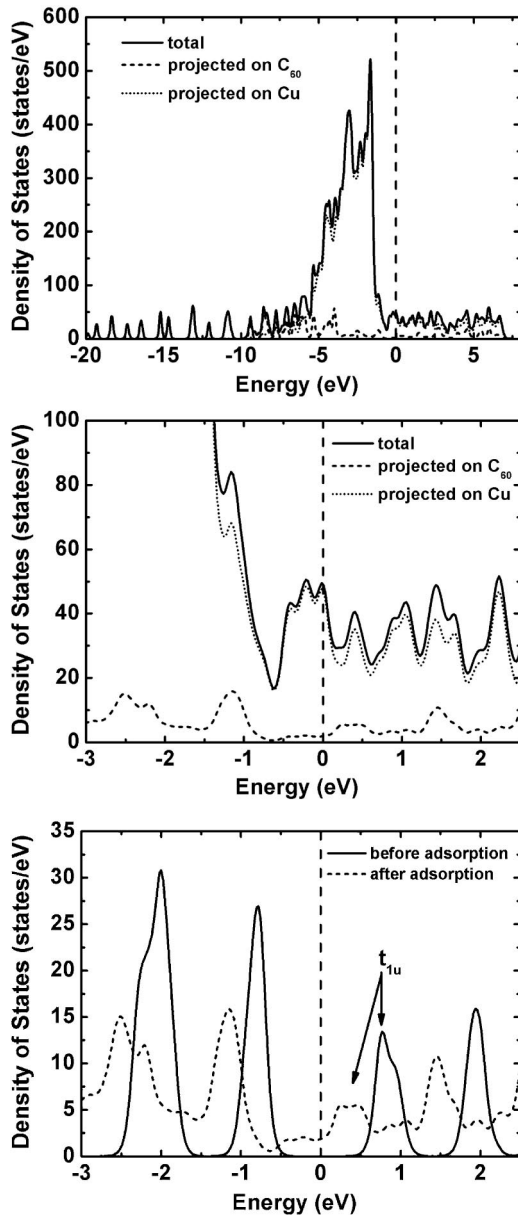
FIG. 3. (a) and (b) DOS and partial DOS of the C_{60}-covered Cu(111) in the full energy range and near the Fermi energy, respectively. (c) Comparison of a C_{60} ML on the surface (dashed line) with an isolated C_{60} ML (solid line).

FIG. 4. Band structure of the C_{60}-Cu(111) system: (a) two bands across a Fermi surface that are likely originated from t_{1u} orbitals; their projections on C_{60} ML are 3% and 13%, respectively. (b) Projection coefficients of bands near the Fermi level on C_{60} (solid line) and Cu slab (dotted line).

compares nicely with experimental results from photoemission spectroscopy.[4] This energy-shift-charge-transfer phenomenon is very characteristic in molecule-surface interactions. It is a compromise between the two systems: A strong bond between the molecule and the surface has formed at the cost of weakening the interaction within both C_{60} and the metal surface.

Integration of the partially filled t_{1u} state leads to a charge transfer $\Delta Q \sim (0.8-0.9)e^-$ per molecule from the copper surface to the C_{60} ML. To confirm the value of ΔQ, a modified Bader approach[38] is used. We first locate the minimum density surface on which $\partial \rho(\mathbf{r})/\partial z = 0$, where $\rho(\mathbf{r})$ is the charge density distribution and z is the direction normal to the Cu surface. Integration of the density above the surface is
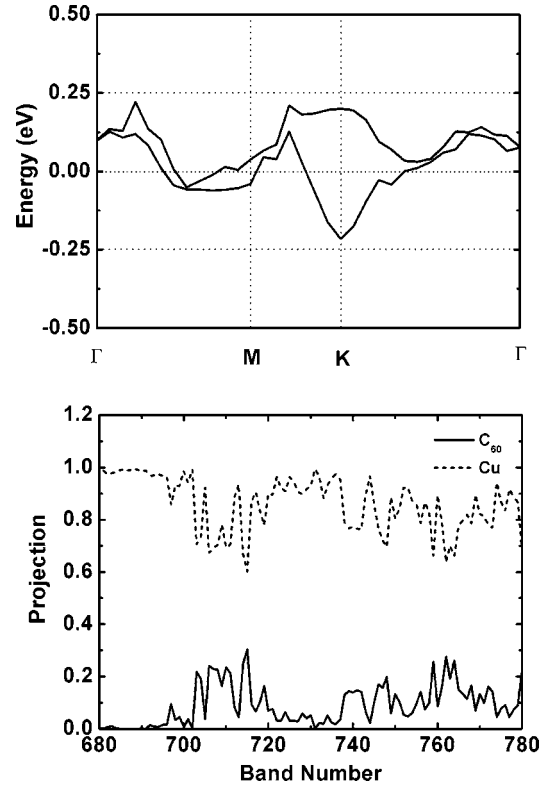
the charge on the molecule and below the charge of the Cu surface. A total $0.8e^-$ charge transfer from the surface to the C_{60} molecule is observed using this analysis.

The band structure of the C_{60}-covered Cu(111) surface indicates a strong band mixing, thus making it difficult to trace the origin of any given band. We select two energy bands that cross the Fermi energy [Fig. 4(a)], which are likely to be bands from the t_{1u} orbital of the C_{60} ML. We found that projections on C_{60} are small fraction compared to the metal surface (only 3% and 13%) along Γ-M-K-Γ. Projections of all bands near the Fermi level are given in Fig. 4(b). It can be seen from these curves that the hybridization between molecular and surface states is significant, indicating strong molecule-surface interactions.

Furthermore, we analyze the DOS for the other sites on the Cu(111) surface (Fig. 5). The DOS is projected on the top Cu layer and on the bottom hexagon in C_{60}. It can be seen that DOS of a fcc site differs very little from the one for the ground state hcp site while the DOS of a on-top site has a quite visible population shift to the right side. Same spectra are also depicted for rotations on the hcp and the on-top sites, respectively. It is known that bonding states, d_{xy}, located at the bottom of d band and the antibonding states, $d_{x^2-y^2}$, are at the top of the d band.[39] Consequently, the population shift to higher (less bonding) or lower energy (more bonding) in DOS reflects the differences in total energy among all the sites and orientation.
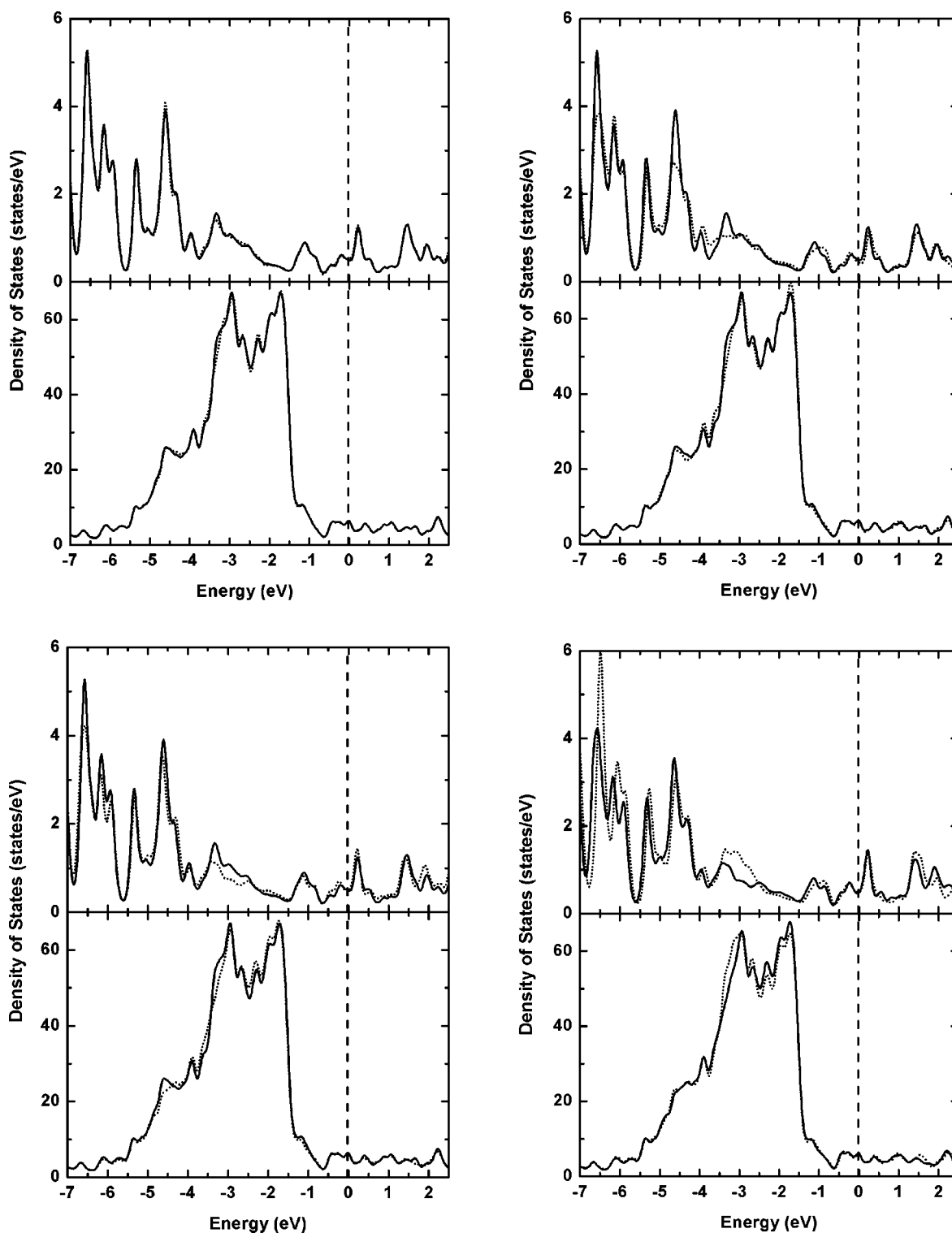
FIG. 5. DOS projected on the bottom hexagon of C_{60} [upper panel in parts (a)–(d)] and on the top surface layer of Cu (111) [lower panel in parts (a)–(d)] for different adsorption sites and orientations. (a) hcp (solid line) vs fcc (dotted line); (b) hcp (solid line) vs on-top (dotted line); (c) hcp (solid line) vs hcp with a 90° rotation (dotted line); and (d) on-top (solid line) vs on-top with a 30° rotation (dotted line).

D. Charge redistribution and work function change

To analyze the charge redistribution, we compute the density difference before and after adsorption according to Eq. (3b). Figure 6 depicts the charge and hole isodensity surfaces for the ground state, i.e., the C_{60} is located in the equilibrium position, and a state in which the C_{60} is almost detached from the surface (a position that is 0.8 Å above the equilibrium). It can be seen that at the equilibrium, the distribution of the electron hole is quite complicated especially in the region between the surface and the molecule [Fig. 6(a)]. The hole
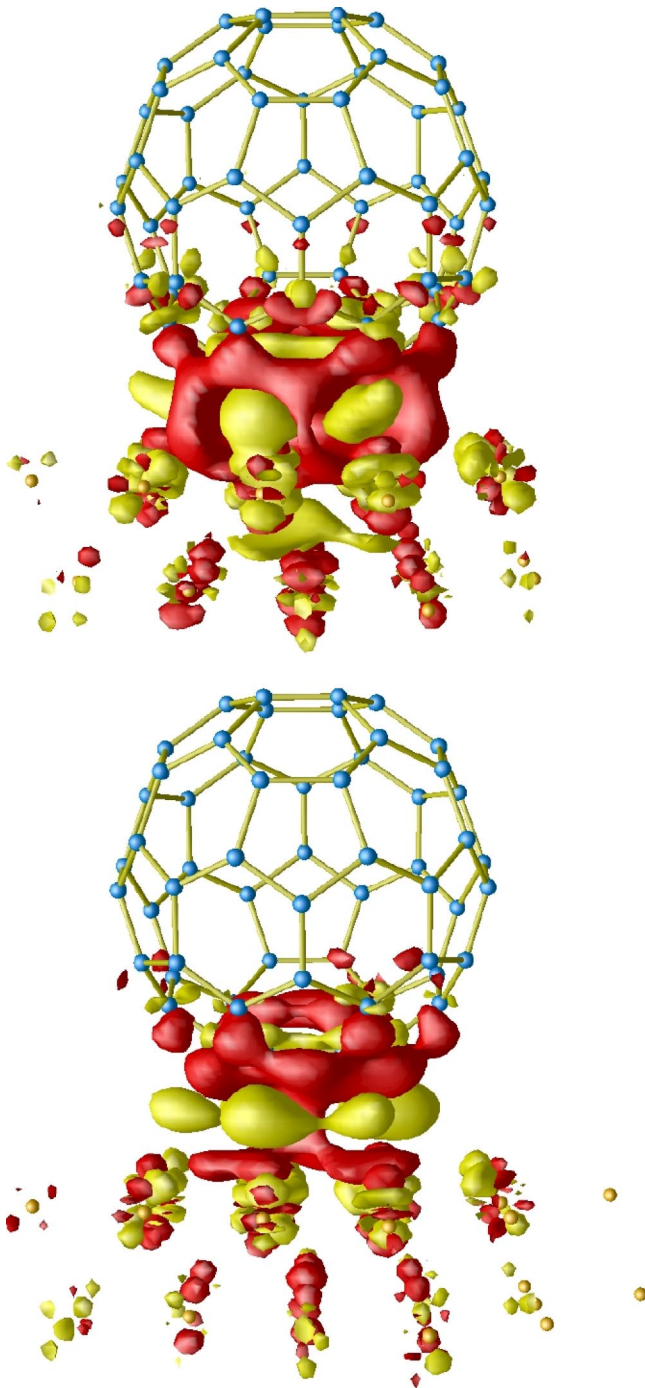
FIG. 7. The planar averaged charge density difference along the direction perpendicular to the surface z. The distance between the bottom hexagon of C_{60} and the top copper layer is 2.0 Å in (a) and 2.8 Å in (b), same as in Fig. 6. The solid vertical lines indicate the positions of the top two copper layers and the dashed lines indicate the locations, in the z direction, of the two parallel boundary hexagons in C_{60}.

FIG. 6. (Color online) Electron (light region) and hole (dark region) isodensity surfaces calculated via Eq. (3c): (a) ground state distribution, (b) the C_{60} molecule is being lifted up by 0.8 Å. The isodensity values are ± 1.0 and $\pm 0.4 e/(10 \times \text{bohr})^3$ in (a) and (b), respectively. The complexity of the distribution shown leads to a net charge transfer from the surface to the ML and a dipole moment that is opposite to the direction of charge transfer.

distribution penetrates into the second Cu layer and somewhat in the C_{60} molecule. When the C_{60} is a little far away from the surface, a clear layered structure is observed [Fig. 6(b)]. This charge redistribution plays an important role in
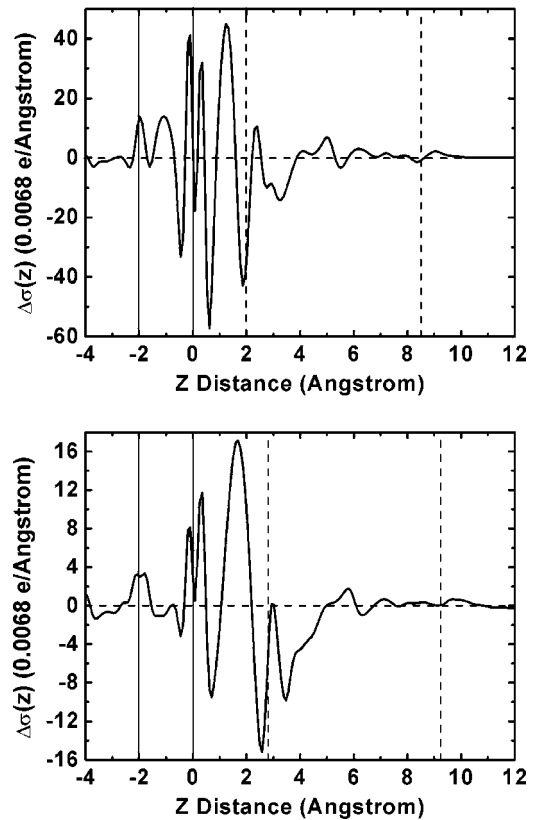
the change of work function, which is related to the surface dipole moment.

The calculated work functions (WF) of a pure Cu(111) surface and C_{60}-covered surface are 5.24 and 5.15 eV, respectively, which are in good agreement with experiments (4.94 and 4.86 eV, respectively).[40] These values are 0.2 eV higher than the experimental values and this is due to the ultrasoft pseudopotential (a test has been performed using Troullier-Martin potential[41,42] with which the calculated WF for Cu(111) surface is 5.0 eV).[43] However, the calculated C_{60}-covered surface does have a work function similar to a clean surface. The calculated WF of a neutral C_{60} ML is 5.74 eV. The WF upon C_{60} adsorption is therefore a combination of a C_{60} ML and a charge transfer from Cu to the C_{60} layer. This result is somewhat puzzling regarding the conventional interpretation of the relationship between the WF change and charge transfer. According to a commonly used analysis[44] based on a simple estimation of dipole moment, when charge transfer occurs from an absorbed molecule to the surface, the WF will decrease; when charge transfer occurs in the other direction, the WF will increase. In our system, a significant charge transfer from the substrate to C_{60} is observed but the WF decreases, although by a tiny amount. To explain this

discrepancy, we use Eq. (3) to evaluate the dipole moment change upon adsorption. Figure 7 demonstrates the planar averaged charge density difference as a function of z. For the ground state, the calculated $\Delta\mu$ is -0.21 D, leading to a change of -0.09 eV in WF, which is in very good agreement with the directly estimated WF and with experiments. When C_{60} is shifted up from its equilibrium by 0.8 Å in the z direction, the calculated charge transfer, change in dipole moment, and work function are $0.2e^-$, -0.73 D, and 4.91 eV (a 0.33 eV decrease), respectively. The calculated WF increase matches perfectly with that derived from the change in dipole moment.

IV. CONCLUSION

In summary, we have presented a detailed microscopic picture of the C_{60}-Cu(111) surface interaction. Large-scale first-principles calculations have provided complete information on the energetics and electronic properties, which govern the structure and dynamical processes observed in experiments. The results are important in understanding the fullerene-metal interfacial characteristics and properties. Especially, the analysis of changes in dipole moment clarifies the puzzling results on work functions. Systematic studies of C_{60} on Al, Ag, and Au surfaces, as well as manipulation of the electronic structure and magnetic properties of these systems by doping are under way.

[1] M. R. C. Hunt *et al.*, Phys. Rev. B **51**, 10 039 (1995).

[2] S. Modesti, S. Cerasari, and P. Rudolf, Phys. Rev. Lett. **71**, 2469 (1993).

[3] A. F. Hebard, R. R. Ruel, and C. B. Eom, Phys. Rev. B **54**, 14 052 (1996).

[4] K.-D. Tsuei *et al.*, Phys. Rev. B **56**, 15 412 (1997).

[5] A. F. Hebard *et al.*, Phys. Rev. B **50**, 17 740 (1994).

[6] A. J. Maxwell *et al.*, Phys. Rev. B **57**, 7312 (1998).

[7] K. L. Akers, L. M. Cousins, and M. Moskovits, Chem. Phys. Lett. **190**, 614 (1992).

[8] S. J. Chase *et al.*, Phys. Rev. B **46**, 7873 (1992).

[9] M. G. Mitch, S. J. Chase, and J. S. Lannin, Phys. Rev. Lett. **68**, 883 (1992).

[10] R. Manaila *et al.*, J. Raman Spectrosc. **30**, 1019 (1999).

[11] A. Rosenberg and D. P. DiLella, Chem. Phys. Lett. **223**, 76 (1994).

[12] D. W. Owens *et al.*, Phys. Rev. B **51**, 17 068 (1995).

[13] L. Firlej, N. Kirova, and A. Zahab, Phys. Rev. B **59**, 16 028 (1999).

[14] M. R. C. Hunt and R. E. Palmer, Philos. Trans. R. Soc. London, Ser. A **356**, 231 (1998).

[15] W. L. Yang *et al.*, Science **300**, 303 (2003).

[16] K. Sakamoto *et al.*, Phys. Rev. B **60**, 2579 (1999).

[17] D. Sanchez-Portal *et al.*, Surf. Sci. **482−485**, 39 (2001).

[18] J. E. Rowe *et al.*, Int. J. Mod. Phys. B **6**, 3909 (1992).

[19] T. Hashizume *et al.*, Phys. Rev. Lett. **71**, 2959 (1993).

[20] C. T. Tzeng *et al.*, Phys. Rev. B **61**, 2263 (2000).

[21] M. Scheffler and A. M. Bradshaw, in *Adsorption at Solid Surfaces*, edited by D. A. K. Woodruff and D. P. Woodruff (Elsevier, Amsterdam, 1983), p. 165.

[22] W. Kohn and L. J. Sham, Phys. Rev. A **140**, 1133 (1965); D. M. Ceperley and B. J. Alder, Phys. Rev. Lett. **45**, 566 (1980); J. P. Perdew and A. Zunger, Phys. Rev. Lett. **23**, 5048 (1981).

[23] D. Vanderbilt, Phys. Rev. B **41**, 7892 (1990).

[24] G. Kresse and J. Furthmuller, Comput. Mater. Sci. **6**, 15 (1996).

[25] H. J. Monkhorst and J. D. Pack, Phys. Rev. B **13**, 5188 (1976).

[26] A. Michaelides *et al.*, Phys. Rev. Lett. **90**, 246103 (2003).

[27] A. D. Becke, Phys. Rev. A **38**, 3098 (1988).

[28] J. P. Perdew and Y. Wang, Phys. Rev. B **45**, 13 244 (1992).

[29] R. W. G. Wyckoff, *Crystal Structure*, 2nd ed. (Interscience, New York, 1963).

[30] R. R. Hultgren, *Selected Values of Thermodymical Properties of Metals and Alloys* (Wiley, New York, 1963).

[31] P. Klooster, N. J. Trappeniers, and S. N. Biswas, Physica B & C **97**, 65 (1979).

[32] P. O. Gartland, S. Berge, and B. J. Slagsvold, Phys. Rev. Lett. **28**, 738 (1972).

[33] S. A. Lindgren *et al.*, Phys. Rev. B **29**, 576 (1984).

[34] A. Fartash, J. Appl. Phys. **79**, 742 (1996).

[35] R. Fasel *et al.*, Phys. Rev. Lett. **76**, 4733 (1996).

[36] T. Hashizume *et al.*, J. Vac. Sci. Technol. A **12**, 2097 (1994).

[37] M. T. Cuberes, R. R. Schlittler, and J. K. Gimzewski, Appl. Phys. A: Solids Surf. **66**, Suppl. 1-2, s669 (1998).

[38] R. F. W. Bader, Chem. Rev. (Washington, D.C.) **91**, 893 (1991).

[39] G. S. Painter, Phys. Rev. B **17**, 3848 (1978).

[40] K. D. Tsuei *et al.*, Phys. Rev. B **56**, 15412 (1997).

[41] N. Troullier and J. L. Martins, Phys. Rev. B **43**, 8861 (1991).

[42] N. Troullier and J. L. Martins, Phys. Rev. B **43**, 1993 (1991).

[43] M. Bockstedte *et al.*, Comput. Phys. Commun. **107**, 187 (1997).

[44] G. Attard and C. Barnes, *Surface* (Oxford University Press, Oxford, 1998).